Joint effects of host genotype and species arrival order govern microbiome composition and function

Devin R. Leopold & Posy E. Busby

Department of Botany and Plant Pathology, Oregon State University

Abstract

There is mounting evidence that species arrival order can affect microbiome composition, a phenomenon known as priority effects. However, it is less clear whether priority effects during microbiome assembly have consequences for the host, or whether intraspecific variation in host traits can alter the trajectory of microbiome assembly. In a greenhouse inoculation experiment, using the *Populus trichocarpa* foliar microbiome, we manipulated host genotype and the arrival order of a synthetic community of foliar fungi. We quantified microbiome assembly outcomes using marker-gene sequencing and tested host susceptibility to a foliar rust pathogen. We found that the effect of species arrival order on microbiome composition and function (i.e., disease modification) depended on host genotype. Additionally, we found that fungal species arrival order can affect host disease susceptibility independent from microbiome composition, suggesting that the interactive effects of species arrival order and host genotype can decouple composition and function in the plant microbiome.

Keywords: community assembly; endophyte; foliar fungi; historical contingency; *Populus trichocarpa*; priority effects; plant microbiome

INTRODUCTION

The species composition of the plant microbiome—the diverse communities of bacteria, fungi, and other microorganisms that live on and in plant tissues—can have significant consequences for plant health and fitness (Vandenkoornhuyse *et al.*, 2015; Busby *et al.*, 2016b; Laforest-Lapointe *et al.*, 2017). Interactions between plants and their microbial symbionts, including pathogens, mutualists, and commensals, over evolutionary time scales have resulted in complex plant innate immune systems that can recognize and respond to signals of microbial colonization (Jones & Dangl, 2006; Dodds & Rathjen, 2010; Hacquard *et al.*, 2017). Other plant traits, such as the production of secondary compounds (Bednarek & Osbourn, 2009; Lebeis *et al.*, 2015), the presence of physical barriers (Reisberg *et al.*, 2013; Bodenhausen *et al.*, 2014), or the active provisioning of resources to beneficial microbial symbionts (Kiers *et al.*, 2011; Huang *et al.*, 2014), also affect the relative abundance of plant associated microbes. As a result of variation in such traits, plant microbiome composition varies among (Redford *et al.*, 2010; Kim *et al.*, 2012) and within plant species (Bressan *et al.*, 2009; Aira *et al.*, 2010; Bálint *et al.*, 2013) and can be viewed as a complex heritable trait. Linking host genetics to plant microbiome composition will provide insight into the evolutionary basis of plant-microbiome interactions while also providing new opportunities in applied plant sciences, such as crop improvement through breeding for more beneficial microbiomes (Bakker *et al.*, 2012; Schlaeppi & Bulgarelli, 2015; Mueller & Sachs, 2015; Busby *et al.*, 2017). However, progress towards these goals is hindered by the fact that the majority of variation in plant microbiome composition often remains unexplained.

One increasingly recognized source of variation in plant microbiome composition is species arrival order and timing during community assembly, a phenomenon known as priority effects (Palmgren, 1926; Sutherland, 1974; Drake, 1991). Priority effects during community assembly have been identified for ecto- and arbuscular mycorrhizal fungi (Kennedy *et al.*, 2009; Werner & Kiers, 2015), nectar microbes (Peay *et al.*, 2012), and bacteria in the foliar microbiome of *Arabidopsis thaliana* (Carlström *et al.*, 2019). However, it is not known whether intraspecific variation in host traits may interact with species arrival order to affect microbiome assembly and function. For example, plant genotypes producing more secondary compounds that inhibit microbial growth may favor more deterministic assembly outcome if they limit which taxa can

establish, or slow the growth rate of early arriving species (Fukami, 2015). In order to make progress towards more generalizable links between plant genes and microbiome composition and function, it is therefore necessary to understand whether and how the joint effects of host genotype and microbial species arrival order affect microbiome community assembly outcomes.

In the plant microbiome, one important function that may be affected by host traits, species arrival order, and their interaction, is the modification of disease severity in the host by non-pathogenic microbes (Spence *et al.*, 2014; Busby *et al.*, 2016b; Zahn & Amend, 2017). For example, fungal endophytes (i.e., non-pathogenic fungi inhabiting plant tissues) isolated from wild lima bean can either enhance plant resistance to an *Enterobacter* pathogen or increase disease susceptibility, depending on arrival order relative to the pathogen (Adame-Álvarez *et al.*, 2014). There is also wide variation in disease modulation among different species, or even isolates, of non-pathogenic microbes, ranging from disease antagonism to disease facilitation (Busby *et al.*, 2013, 2016a). Changes in the relative abundances of these disease-modifying symbionts within the plant microbiome may therefore have implications for plant health. In addition, priming of plant immune response by non-pathogenic microbes can affect subsequent pathogen establishment and disease development (Van Wees *et al.*, 2008; Zamioudis & Pieterse, 2012). In a community context, with many potential direct and indirect interactions between microbial species and the plant (van der Heijden & Hartmann, 2016), complex dynamics are likely to emerge.

Studying priority effects in the plant microbiome is complicated by the fact that species arrival history cannot be inferred *post hoc* from observational data alone. Furthermore, the standard methods for measuring plant microbiome composition (i.e., high-throughput marker gene sequencing) suffer from multiple sources of compounding biases (Brooks, 2016; Sinha *et al.*, 2017) that limit accurate interpretation of changes in species' relative abundance in response to experimental treatments. A tractable approach to overcoming these limitations is to assemble synthetic microbial communities, where immigration history can be precisely controlled (Vorholt *et al.*, 2017; Carlström *et al.*, 2019). In addition, by using a simplified microbial community, with known membership, it is also possible to quantify and correct sequencing biases to more accurately assess community assembly outcomes (McLaren *et al.*, 2019).

In this study, we assembled a synthetic community of 8 foliar fungi commonly associated with the foliar microbiome of the model tree, *Populus trichocarpa* (Busby *et al.*, 2016a; Cregger *et al.*, 2018; Barge *et al.*, 2019), to ask whether interactions between species arrival order (i.e., priority effects) and host genotype (i.e., intraspecific variation) affect fungal community assembly outcomes. To capture intraspecific variation in host traits, we selected *P. trichocarpa* genotypes from populations located on either side of the Cascade Divide, in their native range in northwestern North America (Fig. S1). These regions have distinct climates, with dry, continental conditions prevailing in the east, and wet, relatively mild conditions in the west. *P. trichocarpa* populations from these regions differ in many physical and chemical leaf traits, such as stomatal density and morphology (Dunlap & Stettler, 2001), which are likely to influence community assembly in the foliar microbiome. In addition, *P. trichocarpa* genotypes originating from wetter, western populations experience greater foliar disease pressure and are generally more resistant than eastern genotypes to the widespread foliar rust pathogen, *Melampsora* x *columbiana* (Dunlap *et al.*, 1994; Dunlap & Stettler, 1996; Newcombe *et al.*, 2000).

By factorially manipulating species arrival order and host genotype in a controlled greenhouse experiment, we were able to test hypotheses concerning both compositional and functional outcomes of community assembly in the foliar microbiome. First, we hypothesized that the effect of species arrival order on the relative abundance of foliar fungi would vary among host genotypes, with the greatest differences occurring among genotypes originating from the disparate environments delineated by the Cascade Divide. Second, we hypothesized that differences in immigration history during fungal community assembly would result in varying foliar rust disease severity for rust susceptible, but not rust resistant plant genotypes. And third, we hypothesized that if disease modulation was primarily the result of direct antagonism of the rust pathogen by foliar fungi, variation in rust disease severity would be correlated with fungal community composition.

METHODS

Overview and experimental design

We manipulated the species arrival order of foliar fungi colonizing the leaves of 12 genotypes of the model tree species, *P. trichocarpa*, in a controlled greenhouse experiment. The plant

genotypes originated from populations located both east (5) and west (7) of the Cascade Divide in the northwestern United States (Fig. S1). In the greenhouse, plants were inoculated with a synthetic community of 8 fungal species (Table S1), all isolated from field collected *P. trichocarpa* leaves. Inoculation consisted of two phases: colonization by 1 of 5 randomly selected initial colonists, followed 2 weeks later by inoculation with the full synthetic fungal community. The 5 inoculation treatments, and an additional non-inoculated control treatment, were applied to 5 replicates of 12 clonally propagated *P. trichocarpa* genotypes, resulting in a total of 360 plants. We assessed fungal community assembly outcomes after one month using Illumina sequencing of the nuclear ribosomal, internal transcribed spacer (ITS) region. We then inoculated plants with the foliar rust pathogen *Melampsora* × *columbiana* and assessed disease severity to quantify functional consequences of priority effects in the *P. trichocarpa* foliar microbiome.

Plant propagation

Plants were propagated in a glasshouse on the campus of Oregon State University using dormant hardwood cuttings collected in February 2018, from a common garden. Cuttings were trimmed to *ca.* 10 cm and planted into 550 ml conical Deepots (Stuewe & Sons, Inc.) using commercial potting mix (Sunshine Mix #4) supplemented with 115 ml gal^{-1} slow-release fertilizer (16-6-11+micronutrients). Throughout the experiment, plants were watered from below using an automated sub-irrigation system to keep leaves dry and limit opportunities for colonization by non-target fungi (Huang *et al.*, 2018).

Synthetic fungal community

We isolated foliar fungi from *P. trichocarpa* leaves using standard methods. Briefly, leaf punches were collected into sterile 1.5 ml centrifuge tubes and surface sterilized by sequentially vortexing for 1 minute in 10% bleach (0.825% NaClO), 70% EtOH, and then in 3 consecutive rises in sterile water. We then plated the leaf punches onto potato-dextrose agar, supplemented with penicillin (100 μg ml^{-1}) and streptomycin (100 μg ml^{-1}), and incubated the plates at room temperature for 1 month. Plates were checked daily for fungal growth and emerging hyphae were subcultured using single hyphal-tip isolation. We selected representative morphotypes from the initial culture collection and used Sanger sequencing of the full ITS region for taxonomic identification. We then selected representative isolates of 8 fungal species (Table S1) to use in

our synthetic community of *P. trichocarpa* foliar fungi, which included: *Alternaria alternata*, *Aureobasidium pullulans*, *Cladospoium* sp., *Dioszegia butyracea*, *Epicoccum nigrum*, *Fusarium* sp., *Penicillium bialowiezense*, and *Trichoderma trixiae*. The isolates we selected have been previously identified as common members of the *P. trichocarpa* foliar microbiome (Busby *et al.*, 2016a; Barge *et al.*, 2019). Because definitive species-level identifications from ITS sequence data is not always possible, the genus-level taxonomic assignments will be used to refer to the individual isolates hereafter. Sanger sequences of the full ITS region for the 8 focal species are archived in the NCBI genbank (accession numbers MT035960-7).

Fungal inoculation

We collected fungal inoculum by flooding 2-week old cultures with an aqueous solution of 0.1% Tween 20 and gently scraping the plate surface with a sterile spatula to dislodge conidia, or, in the cases of the yeast-like *Aureobasidium pullans* and the basideomycetous yeast, *Dioszegia* sp., individual cells. We quantified the density of the initial suspension using a hemocytometer and diluted as required using additional sterile 0.1% Tween 20. At the first inoculation time point, we prepared inoculation solutions for each of the 5 initial colonists at a density of 3.3×10^4 cells ml^{-1}. At the second time point, 2 weeks later, inoculation solutions for each treatment were prepared containing each of the 7 other species at a density of 1.0×10^5 cells ml^{-1} and the initial colonist at a density of 6.7×10^4 cells ml^{-1}. As a result, the total amount of inoculum for each species in each treatment was held constant and only the identity of the initial colonist varied. We chose to apply the majority of the inoculum for the initial colonist at the second time point to ensure that differences in assembly outcomes were due to early arrival, and not the absence of the initial colonist from the inoculation solution during colonization by the full community.

Inoculation of plants was achieved by saturating both the top and bottom leaf surfaces with a sterile, fine-mist spray bottle. For each tray holding 12 plants, we applied 75 ml of the inoculum solution and then immediately covered the tray with a temporary humidity tent to maintain leaf surface moisture for 48 hours. Control plants were mock-inoculated using sterile water at both time points. Because *P. trichocarpa* grows rapidly and the experiment was conducted over a period of 6 weeks, we used a wire twist tie to mark the youngest fully expanded leaf at the time of the first inoculation.

Leaf sampling for fungal DNA

From each plant, we collected 4 leaf punches (*ca*. 0.25 cm^2) from each of 3 leaves (12 total) directly into a sterile 1.5 ml centrifuge tube using a standard hole punch, which was cleaned with ethanol between each plant. Leaf disks were placed on ice immediately after collection and processed to remove surface contaminants the same day they were collected. To remove surface contaminants, the leaf disks were agitated for 1 minute in 1 ml of molecular grade water with 0.1% Tween 20, using a Geno/Grinder® 2010, set at 500 strokes per minute. The cleaning solution was remove from the tubes using a sterile pipette and the leaf disks were rinsed by repeating the process 3 times with molecular grade sterile water. The cleaned leaf disks were then frozen at -20 °C and stored until we extracted total genomic DNA using the 96 Well Synergy™ Plant DNA Extraction Kit (OPS Diagnostics). The four corners of each extraction plate were processed without leaf disks to serve as negative controls during library preparation.

Library preparation for ITS metabarcoding

We prepared libraries for Illumina MiSeq metabarcoding, targeting the ITS1 region using a dual-indexed, two-stage PCR approach. In the first PCR, we used modified versions the fungal specific forward gene primer ITS1F (Gardes & Bruns, 1993) and, for the reverse gene primer, the reverse-complement of gITS7 (Ihrmark *et al.*, 2012). Each gene primer was fused with Illumina sequencing primers, separated by a 3-6 bp, degenerate, length-heterogeneity spacer (Lundberg *et al.*, 2013). Stage-one PCR was carried out in 25 µl reactions with MyFi Master Mix (Bioline), 2 µl template DNA, 0.5 µM of each primer and a thermocycling program consisting of an initial denaturing and enzyme activation cycle at 95 °C (3 min.), 32 cycles of 95 °C (30 sec.), 50 °C (30 sec.), and 72 °C (30 sec.), followed by a final elongation cycle at 72 °C (5 min). Temperature ramp rates were limited to 1 °C (Stevens *et al.*, 2013). For each 96-well plate, 2 extraction blanks were included to detect contaminants possibly introduced during DNA extraction and 2 PCR blanks, with no template DNA, were included to detect contamination introduced during library preparation. For stage-two PCR, we used primers that targeted the Illumina sequencing adapters added during stage-one, adding the P5 and P7 Illumina adapters and 8-mer multiplexing barcodes (Hamady *et al.*, 2008). Multiplexing barcodes were selected to have a minimum Hamming distance of 4 and balanced base diversity (Somervuo *et al.*, 2018). Stage-two PCR was carried out in 20 µl reactions with MyFi Master Mix, 1 µl of the stage-one

PCR product as template, 0.5 µM primers, and a thermocycler program consisting of an initial cycle of 95 °C (1 min.), 8 cycles of 95 °C (20 sec.), 55 °C (20 sec.), and 72 °C (30 sec.), followed by a final elongation cycle at 72 °C (5 min). Final PCR products were cleaned and normalized using Just-a-Plate, 96-well normalization and purification plates (Charm Biotech), then pooled and sent to the Oregon State University, Center for Genome Research and Biocomputing, for 250-bp, paired-end sequencing on the Illumina MiSeq platform.

Fungal community bioinformatics

Sequences were demultiplexed with Pheniqs v2.0.4 (Galanti *et al.*, 2017), using a phred-adjusted maximum likelihood confidence threshold of 0.995. Gene primers and length heterogeneity spacers were removed from the 5' ends of the paired reads using cutadapt v1.18 (Martin, 2011), discarding reads with gene primers not found in the expected positions. The 3' ends were trimmed to remove “read-through” adapter contamination using SeqPurge (Sturm *et al.*, 2016). Following trimming, reads were filtered at a maximum expected error rate of 2 bp, denoised, and filtered of putative chimeras using DADA2 (Callahan *et al.*, 2016), with the expected amplicons for the 8 members of the synthetic community included as denoising priors to increase sensitivity. Denoised amplicons were then further collapsed to operational taxonomic units (OTUs) at 99% similarity using agglomerative, single-linkage clustering with the R-package DECIPHER (Wright, Erik, 2016) used to calculate pairwise dissimilarity. Host contamination was removed by filtering the resulting OTUs against the *P. trichocarpa* v3.0 genome (Tuskan *et al.*, 2006) using Bowtie2 (Langmead & Salzberg, 2012). Other likely contaminants were filtered by removing OTUs whose prevalence or mean proportional abundance when present was greater in negative controls. Samples with less than 4000 sequences remaining after all filtering steps were removed from subsequent analyses. The final OTU-by-sample matrix and the sample metadata were combined in a single phyloseq object (McMurdie & Holmes, 2013) for downstream manipulation and analysis in the R v3.6 statistical programming environment (R Core Team, 2019). The raw fastq sequence files are archived in the NCBI Sequence Read Archive (BioProject PRJNA605581) and all bioinformatics scripts and sample meta data have been publicly archived (http://doi.org/10.5281/zenodo.3692043).

Rust disease severity

Immediately following leaf sampling for marker-gene sequencing, we inoculated plants with a rust pathogen. Asexual urediniospores were collected from a single-spore strain of *M.* × *columbiana* being maintained on *P. trichocarpa* plants in an isolated growth chamber. We applied urediniospores at a concentration of 1.0 x 10^4 ml^{-1}, following the same procedure described above. After 2 weeks, we harvested 3 leaves from each plant and photographed the abaxial surface from a fixed distance using a light box. We then used image analysis, with Fiji (Schindelin *et al.*, 2012), to quantify rust disease severity. First, we isolated leaves from the image background and quantified total leaf area using color thresholding. We then used supervised image segmentation (Arganda-Carreras *et al.*, 2017) to quantify the proportion each leaf occupied by either chlorotic lesions or rust uredinia, to related measures of rust disease severity.

Estimating sequencing bias

To quantify and correct for species-specific sequencing biases introduced during Illumina library preparation and sequencing, we constructed mock communities with known abundances of fungal DNA that were sequenced along with our experimental samples. To assemble the mock communities, we first extracted genomic DNA from pure cultures of each of the 8 members of the synthetic community and the rust pathogen using the *Quick*-DNA Fungal/Bacterial Miniprep Kit (Zymo Research). We then used Sanger sequencing and Primer 3 (Untergasser *et al.*, 2012) to design custom qPCR primers to quantify the concentrations of our pure culture extracts. We targeted the TEF1-α gene for qPCR quantification because it is a single-copy gene, unlike the ITS region, which can vary in copy number among fungi over several orders of magnitude (Lofgren *et al.*, 2019), likely representing a large source of bias in fungal ITS metabarcoding. Absolute qPCR quantification was carried out using PowerUP SYBR Master Mix (Applied Biosystems) and the 7500 Fast Real-Time PCR System (Applied Biosystems). We then used the qPCR estimated concentrations of the single culture extracts to combine genomic DNA for each species in 10 different mock communities, each containing all 9 fungal species. For 1 mock community, all species were present in equal concentrations (5 x 10^4 copies μl^{-1}). For the remaining 9 mock communities, species were added at either, 1 x 10^4 copies μl^{-1}, 5 x 10^4 copies μl^{-1}, or 2.5 x 10^5 copies μl^{-1}. Each species was present at each concentration in 3 mock communities and all 9 mock communities had 3 species at each concentration. The resulting

mock community samples were prepared for Illumina sequencing in parallel with the experimental samples following the protocol outlined above.

Sequencing read counts and the known proportional abundances of each species in each mock community were then used to estimate species-specific biases following the method of (McLaren *et al.*, 2019). We found significant bias among the members of our mock communities (Figs. S2 & S3), with *M.* x *columbiana*, having the greatest positive bias, being over represented relative to the most negatively biased species, *Penicillium* sp. by a factor of 40. Among the members of our synthetic community of foliar fungi, the most positively biased species was *Fusarium* sp., which was over represented relative to *Penicillium* sp. by a factor of 13. Use of the estimated bias correction factors to account for sequencing bias is described in the data analysis section below.

Data analysis

To assess whether the community assembly of *P. trichocarpa* foliar fungi was influenced by the 5 colonization order treatments, 12 host genotypes, and their interaction, we fit a multivariate, negative-binomial glm, using the R-package mvabund (Wang *et al.*, 2019). We accounted for 2 sources of unequal sampling effort, variable sampling depth and the species-specific sequencing biases, by including an offset term (*effort*) for each species *i* in each sample *j*, in the form: $effort_{ij} = \log(bias_i \times depth_j)$, where $bias_i$ is the sequencing bias correction factor for species *i*, estimated from our mock communities (see above, *Estimating Sequencing Bias*), and $depth_j$ is the total sum of all species in sample *j*, after dividing each by their species-specific sequencing bias correction factor. We used Wald tests to asses the significance of model terms, accounting for non-independence of species relative abundances by estimating a species correlation matrix (Warton, 2011) and by assessing significance using permutation tests, while maintaining species correlations, to calculate p-values (Warton *et al.*, 2017). To determine whether geographic origin (i.e., east or west of the Cascade Divide) explained the observed effects of host genotype, we fit a second multivariate glm with plant genotype re-coded as a binary factor (east or west). We visualized the multivariate effects of our experimental treatments using distance-based redundancy analysis, in the R-package vegan (Oksanen *et al.*, 2017), using Wisconsin Double Standardization and Jensen-Shannon Distance between samples as a measure of community dissimilarity.

We used two approaches to determine the relative contributions of individual species to the overall variation in community composition in response to our experimental treatments. First, we extracted univariate test statistics from our multivariate glms, using permutation tests and step-down resampling to control the family-wise error rates. To quantify univariate effect sizes, we fit individual negative-binomial glms for each species with the R-package MASS (Venables & Ripley, 2002), and estimated the partial-R^2 for each model term, following the method of (Nagelkerke, 1991).

As an alternative approach to assessing the impact of the experimental treatments on individual species, we quantified the benefit of preemptive colonization (i.e., priority effects) for each of the 5 initial colonists. For each initial colonist on each host genotype, we defined the strength of priority effects as the log-ratio of the mean proportional abundance when arriving first to the mean proportional abundance when arriving concurrent with the community, following (Vannette & Fukami, 2014). This calculation results in positive values if the relative abundance was greater when the species arrived before the community. We calculated point estimates for the strength of the priority effect for each species on each host genotype, using bootstrapping to estimate confidence intervals, randomly sampling with replacement 10,000 times for each treatment combination and recalculating the strength of the priority effect for each iteration. Bias-corrected and accelerated confidence intervals (DiCiccio & Efron, 1996) were estimated from the resulting distributions. To test whether each species experienced significant priority effects on plant genotypes originating from eastern or western populations overall, we used bootstrapped one-sample t-tests. To ensure that the bootstrapping process resembled the data generation process, we used a two-stage resampling procedure, beginning with the 10,000 bootstrapped point-estimates of priority effects describe above. For each set of bootstrapped point estimates, we drew 100 bootstrap samples for each species and host region of origin (eastern or western) combination and calculated the t-statistic under the null hypothesis of no difference in relative abundance due to arrival timing. The bootstrapped, one-tailed p-values were then calculated as the proportion of times the bootstrapped t-statistics were greater than the values from the observed data.

We then tested whether our experimental treatments affected the severity of leaf rust disease, measured as the proportion of leaf surface occupied by chlorotic lesions or rust uredinia,

averaged over three leaves per plant. We separated highly resistant and susceptible genotypes for this analysis because our disease severity data indicated 2 qualitatively distinct groups, one of which likely posses major-gene resistance to the rust pathogen (Duplessis *et al.*, 2009; Hacquard *et al.*, 2011), precluding variation in disease severity (Fig. S4). For each group, we then fit generalized linear models with a beta distribution (i.e., beta-regression), using the R-package betareg (Cribari-Neto & Zeileis, 2010). To account for the presence of zeros in the rust uredinia data, a transformation was applied, following (Smithson & Verkuilen, 2006), $(y * (n - 1) + 0.5) / n$, where y is the proportion of leaf with rust uredinia and n is the total number of plants sampled. In addition, because some indiviudal leaves were lost during handling, we accounted variation in measurement precision by using the number of leaves sampled per plant as proportionality weights in the models. To determine whether host genotype and fungal species arrival order interactively determined disease severity, we compared models with and without an interaction term using likelihood-ratio tests, implemented with the R-package lmtest (Zeileis & Hothorn, 2002). We then tested the marginal direct effects of host genotype and species arrival order on disease severity. Analyses of both measures of rust disease severity, chlorotic lesions and uredinia, yielded identical conclusions, so we present only the former.

We then tested whether variation in disease severity within each susceptible plant genotype could be explained by variation in the relative abundance of individual foliar fungi, or community-level variation associated with the species arrival order treatments. First, we fit a new beta-regression model to the rust severity data with only host genotype as a predictor. We then extracted the standardized residuals to use as a new response variable capturing variation in disease severity after accounting for differences among individual plant genotypes. To assess whether residual rust severity was related to the relative abundance of individual foliar fungi, we then conducted Pearson's correlation tests and examined scatter plots, using log-odds transformed proportional fungal abundance. To assess whether residual rust severity was associated with the species arrival order treatment effects on overall fungal community composition, we first conducted a distance based redundancy analysis of fungal community dissimilarity, using Jensen-Shannon Distance, and conditioned on host genotype effects, to identify orthogonal axes of variation associated species arrival order. We then used Pearson's correlation tests and examined scatter plots, as above.

All analyses were conducted using R v3.6.2 (R Core Team, 2019) and all code and raw data to reproduce the analyses has been publicly archived (http://doi.org/10.5281/zenodo.3692043).

RESULTS

Fungal species composition

In support of our first hypothesis, we found that fungal species composition of the *P. trichocarpa* foliar microbiome depended on species arrival order (Wald-$\chi^2_{(4)} = 21.8$, $P < 0.001$; Fig. 1a), and that the effect of arrival order varied across plant genotypes (Wald-$\chi^2_{(44)} = 23.5$, $P = 0.04$). The direct effect of plant genotype on fungal species composition (Wald-$\chi^2_{(11)} = 20.2$, $P < 0.001$) was partially explained by whether the genotype originated east or west of the Cascade Divide (Wald-$\chi^2_{(1)} = 12.4$, $P < 0.001$; Fig. 1b; Fig. S5). However, contrary to our expectation, we did not find evidence that the effect of species arrival order on fungal community composition was systematically influenced by the geographic origin of the host (Wald-$\chi^2_{(4,238)} = 6.16$, $P = 0.31$; Fig. S6).

Community-level variation in fungal species composition (Fig. 1; Table 1) was the result of differing responses of individual fungi to the experimental design, with some species responding more strongly to arrival order and others responding more strongly to host genotype (Fig. 2). The effect of species arrival order was not limited to taxa that served as initial colonists, indicating that the identity of the initial colonist can result in complex indirect effects on the trajectory of community assembly. However, we did not find strong evidence that the effect of species arrival order on the relative abundance of each of the eight community members varied among host genotypes; an effect which only became evident for the community as a whole (Table 1). In addition, while the relative abundances of the 5 early arriving species all varied among arrival order treatments (Fig. 2), not all species consistently benefited from preemptive colonization on all genotypes (Fig. 3). Although we did observe considerable variation in the strength of priority effects for the individual early arriving species across host genotypes, these effects could not be attributed to the geographic origin of the plant (Fig. 3).

Rust disease severity

In support of our second hypothesis, the effect of fungal species arrival order on rust disease severity depended on whether the host genotype was susceptible or resistant to the rust pathogen

(Table 2). Specifically, for susceptible, primarily eastern genotypes, disease severity depended on the interaction between fungal species arrival order and host genotype (LRT-$\chi^2_{(20)}$ = 33.6, P = 0.03; Fig. 4). However, while there was variation in the overall level of rust disease observed among the highly rust resistant, primarily western genotypes (LRT-$\chi^2_{(5)}$ = 33.5, P < 0.001), the arrival order of foliar fungi did not affect rust disease development (LRT-$\chi^2_{(20)}$ = 1.74, P = 0.78; Fig. S7).

We did not find evidence to support our third hypothesis, that rust disease severity could be explained by the relative abundance of any individual foliar fungi or the overall fungal community response to species arrival order treatments (Fig. S8).

DISCUSSION

Our results demonstrate that the consequences of priority effects in the *P. trichocarpa* foliar microbiome are shaped by genotype specific traits of the host. The interactive effects of species arrival order and host genotype impacted both the composition of the fungal community and the severity of foliar rust disease. For species composition, the interactive effects of host genotype and species arrival order were subtle and could not be explained by differences in host genotypes originating from the distinct environments, east and west of the Cascades. In contrast, the effect of species arrival order on the severity of foliar rust disease was dependent on the plants' intrinsic rust disease resistance. Furthermore, variation in rust disease severity in susceptible plants was not correlated with fungal species composition, suggesting that the functional outcomes of community assembly under priority effects can be decoupled from species composition in the foliar microbiome.

Species composition

Although the effect of fungal species arrival order on foliar microbiome composition varied across *P. trichocarpa* genotypes, community assembly outcomes under priority effects could not be predicted by the geographic origin of the host. This suggests that the plant traits that interact with species arrival order to affect community assembly are not those physical leaf traits that broadly segregate across the wet and dry regions sampled. It is possible that other traits with greater variance among individual *P. trichocarpa* genotypes, such as those involved in microbial recognition and immune response signaling (Duplessis *et al.*, 2009; Zhang *et al.*, 2019; Kainer *et*

al., 2020), are responsible for the genotype-by-arrival order interaction we observed. However, experiments across many more genotypes, using genome wide association analyses, would be needed to test this hypothesis (Wallace *et al.*, 2018).

Variation in the identity of the initial colonist affected the relative abundances of all but one member of the synthetic community of foliar fungi, yet, only 3 of the 5 early arriving species consistently experienced a benefit from preemptive colonization (Fig. 3). This could be the result of intrinsic fitness differences among the initial colonists, or differences in their niche overlap with the other community members, affecting the benefit of early arrival (Ke & Letten, 2018). For example, *Alternaria* had the greatest relative abundance across all treatments and, although it did benefit from early arrival, the magnitude of the observed priority effect for this species was relatively low. This could suggest that *Alternaria* is competitively dominant within the foliar microbiome, limiting the possibility of niche preemption by other species, though we cannot rule out the possibility that this species occupies a distinct niche within the leaf. Niche differences, such as specialization on the leaf surface vs. interstitial space would also reduce the relative importance of arrival order and could explain why species that did not benefit from early arrival often varied in relative abundance in response to the identity of other initial colonists. Future efforts to identify the specific axes of niche differentiation that best explain priority effects in the plant microbiome will help advance the development of more general plant microbiome assembly rules (Vannette & Fukami, 2014).

Rust disease severity

Although we found that species arrival order affected disease severity in rust susceptible plant genotypes, we did not find evidence that this was the result of consistent shifts in the relative abundance of individual fungi. One explanation for this could be that disease modification by early arriving species occurred primarily through interaction with the plant's immune system (Van Wees *et al.*, 2008; Zamioudis & Pieterse, 2012), decoupling the outcome of microbiome community assembly from disease development. Alternatively, disease modification may be the result of complex direct and indirect interactions with the entire fungal community, not individual species. Although some individual foliar fungi can have large effects on *P. trichocarpa* foliar rust severity (Busby *et al.*, 2016a), we did not pre-screen the fungi used in this experiment to select species that were associated with disease modulation effects. Including such

species in our synthetic communities may have yielded stronger links between fungal community composition and rust disease.

Limitations and future directions

Standard approaches to marker-gene sequencing of microbiome communities only provide data on the relative abundances of taxa within each sample, i.e., compositional data (Gloor *et al.*, 2016; Quinn *et al.*, 2018). It is possible that total fungal abundance in the foliar microbiome varies among plant genotypes due to variation in resource availability, leaf thickness, or other leaf traits (Guo *et al.*, 2020). Variation in total fungal abundance could be consequential for disease modulation, particularly if direct pathogen antagonism by non-pathogenic microbes contributes to disease suppression. Variation in total microbial abundance could also have implications for priority effects during microbiome community assembly. Specifically, priority effects should be more important when the community size is limited by space or resources because niche preemption by early arriving species is more likely (Fukami, 2004; Orrock & Fletcher, 2005). However, priority effects may be stronger in resource rich environments if the growth rate of early arriving species is increased (Chase, 2010; Kardol *et al.*, 2013), though greater local resource availability can reduce the strength of priority effects in fungi by reducing the rate of substrate exploration (Leopold *et al.*, 2017). Progress towards understanding the interactive effects species arrival order and host genotype on plant microbiome composition and function will require quantitative data on microbial abundance.

Given the scale of the current study, it was not possible to link individual plant genes or traits with fungal community assembly under priority effects. However, many layers of phenotypic and genotypic data have been collected for more than 1000 re-sequenced *P. trichocarpa* genotypes (Tuskan *et al.*, 2006; Weighill *et al.*, 2018). In the future, research with the *P. trichocarpa* foliar microbiome could leverage these rich data sets to link host traits to priority effects during microbiome assembly. Furthermore, the role of stochastic dispersal timing represents only one of many higher-level processes regulating the assembly of microbial communities (Nemergut *et al.*, 2013). Linking host genotypic variation to these high-level processes is likely to yield generalizable insights into plant regulation of microbiome composition and function.

CONCLUSIONS

In a recent study, Carlström *et al.* (2019) used experimental manipulations of a synthetic community of *Arabidopsis thaliana* phyllosphere bacteria to demonstrate that colonization timing has important consequences for community assembly outcomes in the foliar microbiome. Our study builds on this important work in a number of ways. First, we have shown that host genotype and species arrival order interact to determine the trajectory of microbiome community assembly. This finding suggests that the effects of species arrival order and timing are mediated by host traits, and that future efforts should aim to identify these traits to work towards truly generalizable microbiome community assembly rules. Second, we have shown that the disease modulation function of the foliar microbiome can be affected by species arrival order, and that this effect may be decoupled from microbiome composition. This finding raises intriguing questions about the direct and indirect interaction networks that may underlay disease modulation by foliar fungi. Addressing these complex questions will require emerging computational approaches that merge the multiple layers of omics networks that are increasingly available for model plants, such as *P. trichocarpa* (e.g., Furches *et al.*, 2019). Third, our study has demonstrated the feasibility of controlled manipulations of fungal community assembly in the phyllosphere using a tractable synthetic community. While manipulations of synthetic plant microbiomes is increasingly seen as a valuable experimental approach, most efforts have focused on bacteria (Bodenhausen *et al.*, 2014; Vorholt *et al.*, 2017), while fungi are often the most functionally prominent symbionts associated with plants (Christian *et al.*, 2015). Future manipulative experiments using synthetic fungal communities will be necessary to establish the foundational knowledge needed to realize the promise of selective manipulation of plant microbiome assembly for applications in agriculture or natural resource management.

ACKNOWLEDGMENTS

We are grateful to Bruce McCune, George Newcombe, and Maggie R. Wagner for feedback during the preparation of this manuscript. This research was supported by the US Department of Energy's Office of Biological and Environmental Research (DE-SC0019435) and by the Oregon State University, Department of Botany and Plant Pathology.

AUTHOR CONTRIBUTIONS

DRL lead all aspects of the planning and implementation of the experiment, data collection and analysis, and manuscript preparation, with input and contributions from PEB at all stages.

Data availability

Raw sequence data for this project can be found in the NCBI Sequence Read Archive (BioProject PRJNA605581). Additional sample data is available in the archived code repository (http://doi.org/10.5281/zenodo.3692043).

Code availability

A GitHub repository containing all code required to reproduce the analyses presented in this manuscript, as well as associated sample metadata, has been publicly archived (http://doi.org/10.5281/zenodo.3692043). No unpublished algorithms or methods were used.

References

Adame-Álvarez R-M, Mendiola-Soto J, Heil M. **2014**. Order of arrival shifts endophyte-pathogen interactions in bean from resistance induction to disease facilitation. *FEMS Microbiology Letters* **355**: 100–107.

Aira M, Gómez-Brandón M, Lazcano C, Bååth E, Domínguez J. **2010**. Plant genotype strongly modifies the structure and growth of maize rhizosphere microbial communities. *Soil Biology and Biochemistry* **42**: 2276–2281.

Arganda-Carreras I, Kaynig V, Rueden C, Eliceiri KW, Schindelin J, Cardona A, Sebastian Seung H. **2017**. Trainable Weka Segmentation: a machine learning tool for microscopy pixel classification. *Bioinformatics* **33**: 2424–2426.

Bakker MG, Manter DK, Sheflin AM, Weir TL, Vivanco JM. **2012**. Harnessing the rhizosphere microbiome through plant breeding and agricultural management. *Plant and Soil* **360**: 1–13.

Bálint M, Tiffin P, Hallström B, O'Hara RB, Olson MS, Fankhauser JD, Piepenbring M, Schmitt I. **2013**. Host genotype shapes the foliar fungal microbiome of balsam Poplar (*Populus balsamifera*). *PLoS ONE* **8**: e53987.

Barge EG, Leopold DR, Peay KG, Newcombe G, Busby PE. **2019**. Differentiating spatial from environmental effects on foliar fungal communities of *Populus trichocarpa*. *Journal of Biogeography* **46**: 2001–2011.

Bednarek P, Osbourn A. **2009**. Plant-microbe interactions: chemical diversity in plant defense. *Science* **324**: 746–748.

Bodenhausen N, Bortfeld-Miller M, Ackermann M, Vorholt JA. **2014**. A synthetic community approach reveals plant genotypes affecting the phyllosphere microbiota. *PLoS Genetics* **10**: e1004283.

Bressan M, Roncato M, Bellvert F, Comte G, Haichar F el Z, Achouak W, Berge O. **2009**. Exogenous glucosinolate produced by *Arabidopsis thaliana* has an impact on microbes in the rhizosphere and plant roots. *The ISME Journal* **3**: 1243–1257.

Brooks JP. **2016**. Challenges for case-control studies with microbiome data. *Annals of Epidemiology* **26**: 336-341.e1.

Busby PE, Peay KG, Newcombe G. **2016a**. Common foliar fungi of *Populus trichocarpa* modify Melampsora rust disease severity. *New Phytologist* **209**: 1681–1692.

Busby PE, Ridout M, Newcombe G. **2016b**. Fungal endophytes: modifiers of plant disease. *Plant Molecular Biology* **90**: 645–655.

Busby PE, Soman C, Wagner MR, Friesen ML, Kremer J, Bennett A, Morsy M, Eisen JA, Leach JE, Dangl JL. **2017**. Research priorities for harnessing plant microbiomes in sustainable agriculture. *PLOS Biology* **15**: e2001793.

Busby PE, Zimmerman N, Weston DJ, Jawdy SS, Houbraken J, Newcombe G. **2013**. Leaf endophytes and *Populus* genotype affect severity of damage from the necrotrophic leaf pathogen, *Drepanopeziza populi*. *Ecosphere* **4**: art125.

Callahan BJ, McMurdie PJ, Rosen MJ, Han AW, Johnson AJA, Holmes SP. **2016**. DADA2: High-resolution sample inference from Illumina amplicon data. *Nature Methods* **13**: 581–583.

Carlström CI, Field CM, Bortfeld-Miller M, Müller B, Sunagawa S, Vorholt JA. **2019**. Synthetic microbiota reveal priority effects and keystone strains in the *Arabidopsis* phyllosphere. *Nature Ecology & Evolution* **3**: 1445–1454.

Chase JM. **2010**. Stochastic community assembly causes higher biodiversity in more productive environments. *Science* **328**: 1388–1391.

Christian N, Whitaker BK, Clay K. **2015**. Microbiomes: unifying animal and plant systems through the lens of community ecology theory. *Frontiers in Microbiology* **6**: 1–15.

Cregger MA, Veach AM, Yang ZK, Crouch MJ, Vilgalys R, Tuskan GA, Schadt CW. **2018**. The Populus holobiont: dissecting the effects of plant niches and genotype on the microbiome. *Microbiome* **6**: 31.

Cribari-Neto F, Zeileis A. **2010**. Beta Regression in R. *Journal of Statistical Software* **34**: 1–24.

DiCiccio T, Efron B. **1996**. Bootstrap confidence intervals. *Statistical Science* **11**: 189–212.

Dodds PN, Rathjen JP. **2010**. Plant immunity: towards an integrated view of plant–pathogen interactions. *Nature Reviews Genetics* **11**: 539–548.

Drake J. **1991**. Community-assembly mechanics and the structure of an experimental species ensemble. *American Naturalist* **137**: 1–26.

Dunlap JM, Heilman PE, Stettler RF. **1994**. Genetic variation and productivity of *Populus trichocarpa* and its hybrids. VII. Two-year survival and growth of native black cottonwood clones from four river valleys in Washington. *Canadian Journal of Forest Research* **24**: 1539–1549.

Dunlap JM, Stettler RF. **1996**. Genetic variation and productivity of *Populus trichocarpa* and its hybrids. IX. Phenology and *Melampsora* rust incidence of native black cottonwood clones from four river valleys in Washington. *Forest Ecology and Management* **87**: 233–256.

Dunlap JM, Stettler RF. **2001**. Variation in leaf epidermal and stomatal traits of *Populus trichocarpa* from two transects across the Washington Cascades. *Canadian Journal of Botany* **79**: 528–536.

Duplessis S, Major I, Martin F, Séguin A. **2009**. Poplar and pathogen interactions: insights from *Populus* genome-wide analyses of resistance and defense gene families and gene expression profiling. *Critical Reviews in Plant Sciences* **28**: 309–334.

Fukami T. **2004**. Assembly history interacts with ecosystem size to influence species diversity. *Ecology* **85**: 3234–3242.

Fukami T. **2015**. Historical contingency in community assembly: integrating niches, species pools, and priority effects. *Annual Review of Ecology, Evolution, and Systematics* **46**: 1–23.

Furches A, Kainer D, Weighill D, Large A, Jones P, Walker AM, Romero J, Gazolla JGFM, Joubert W, Shah M, *et al.* 2019. Finding new cell wall regulatory genes in *Populus trichocarpa* using multiple lines of evidence. *Frontiers in Plant Science* **10**: 1–17.

Galanti L, Shasha D, Gunsalus K. **2017**. Pheniqs: fast and flexible quality-aware sequence demultiplexing. *bioRxiv*: 128512.

Gardes M, Bruns TD. **1993**. ITS primers with enhanced specificity for basidiomycetes - application to the identification of mycorrhizae and rusts. *Molecular ecology* **2**: 113–8.

Gloor GB, Macklaim JM, Vu M, Fernandes AD. **2016**. Compositional uncertainty should not be ignored in high-throughput sequencing data analysis. *Austrian Journal of Statistics* **45**: 73.

Guo X, Zhang X, Qin Y, Liu Y-X, Zhang J, Zhang N, Wu K, Qu B, He Z, Wang X, *et al.* 2020. Host-associated quantitative abundance profiling reveals the microbial load variation of root microbiome. *Plant Communications* **1**: 100003.

Hacquard S, Petre B, Frey P, Hecker A, Rouhier N, Duplessis S. **2011**. The Poplar-Poplar rust interaction: insights from genomics and transcriptomics. *Journal of Pathogens* **2011**: 1–11.

Hacquard S, Spaepen S, Garrido-Oter R, Schulze-Lefert P. **2017**. Interplay between innate immunity and the plant microbiota. *Annual Review of Phytopathology* **55**: 565–589.

Hamady M, Walker JJ, Harris JK, Gold NJ, Knight R. **2008**. Error-correcting barcoded primers for pyrosequencing hundreds of samples in multiplex. *Nature Methods* **5**: 235–237.

van der Heijden MGA, Hartmann M. **2016**. Networking in the plant microbiome. *PLOS Biology* **14**: e1002378.

Huang X-F, Chaparro JM, Reardon KF, Zhang R, Shen Q, Vivanco JM. **2014**. Rhizosphere interactions: root exudates, microbes, and microbial communities. *Botany* **92**: 267–275.

Huang Y-L, Zimmerman N, Arnold A. **2018**. Observations on the early establishment of foliar endophytic fungi in leaf discs and living leaves of a model woody angiosperm, *Populus trichocarpa* (Salicaceae). *Journal of Fungi* **4**: 58.

Ihrmark K, Bödeker ITM, Cruz-Martinez K, Friberg H, Kubartova A, Schenck J, Strid Y, Stenlid J, Brandström-Durling M, Clemmensen KE, *et al.* 2012. New primers to amplify the fungal ITS2 region--evaluation by 454-sequencing of artificial and natural communities. *FEMS microbiology ecology* **82**: 666–77.

Jones JDG, Dangl JL. **2006**. The plant immune system. *Nature* **444**: 323–329.

Kainer D, Hyatt PD, Jones P, Streich J, Shah M, Ranjan P, Chen J. **2020**. The *Populus trichocarpa* pan-genome provides insights into the function of gene presence and absence variation. *Nature Genetics* **In press**.

Kardol P, Souza L, Classen AT. **2013**. Resource availability mediates the importance of priority effects in plant community assembly and ecosystem function. *Oikos* **122**: 84–94.

Ke P-J, Letten AD. **2018**. Coexistence theory and the frequency-dependence of priority effects. *Nature Ecology & Evolution* **2**: 1691–1695.

Kennedy PG, Peay KG, Bruns TD. **2009**. Root tip competition among ectomycorrhizal fungi: are priority effects a rule or an exception? *Ecology* **90**: 2098–2107.

Kiers ET, Duhamel M, Beesetty Y, Mensah J a, Franken O, Verbruggen E, Fellbaum CR, Kowalchuk G a, Hart MM, Bago A, *et al.* 2011. Reciprocal rewards stabilize cooperation in the mycorrhizal symbiosis. *Science* **333**: 880–2.

Kim M, Singh D, Lai-Hoe A, Go R, Abdul Rahim R, A.N. A, Chun J, Adams JM. **2012**. Distinctive phyllosphere bacterial communities in tropical trees. *Microbial Ecology* **63**: 674–681.

Laforest-Lapointe I, Paquette A, Messier C, Kembel SW. **2017**. Leaf bacterial diversity mediates plant diversity and ecosystem function relationships. *Nature* **546**: 145–147.

Langmead B, Salzberg SL. **2012**. Fast gapped-read alignment with Bowtie 2. *Nature Methods* **9**: 357–359.

Lebeis SL, Paredes SH, Lundberg DS, Breakfield N, Gehring J, McDonald M, Malfatti S, Glavina del Rio T, Jones CD, Tringe SG, *et al.* 2015. Salicylic acid modulates colonization of the root microbiome by specific bacterial taxa. *Science* **349**: 860–864.

Leopold DR, Wilkie JP, Dickie IA, Allen RB, Buchanan PK, Fukami T. **2017**. Priority effects are interactively regulated by top-down and bottom-up forces: evidence from wood decomposer communities. *Ecology Letters* **20**: 1054–1063.

Lofgren LA, Uehling JK, Branco S, Bruns TD, Martin F, Kennedy PG. **2019**. Genome-based estimates of fungal rDNA copy number variation across phylogenetic scales and ecological lifestyles. *Molecular Ecology* **28**: 721–730.

Lundberg DS, Yourstone S, Mieczkowski P, Jones CD, Dangl JL. **2013**. Practical innovations for high-throughput amplicon sequencing. *Nature Methods* **10**: 999–1002.

Martin M. **2011**. Cutadapt removes adapter sequences from high-throughput sequencing reads. *EMBnet.journal* **17**: 10.

McLaren MR, Willis AD, Callahan BJ. **2019**. Consistent and correctable bias in metagenomic sequencing experiments. *eLife* **8**: 559831.

McMurdie PJ, Holmes S. **2013**. phyloseq: An R package for reproducible interactive analysis and graphics of microbiome census data. *PLoS ONE* **8**: e61217.

Mueller UG, Sachs JL. **2015**. Engineering microbiomes to improve plant and animal health. *Trends in Microbiology* **23**: 606–617.

Nagelkerke NJD. **1991**. A note on a general definition of the coefficient of determination. *Biometrika* **78**: 691–692.

Nemergut DR, Schmidt SK, Fukami T, O'Neill SP, Bilinski TM, Stanish LF, Knelman JE, Darcy JL, Lynch RC, Wickey P, *et al.* 2013. Patterns and processes of microbial community assembly. *Microbiology and Molecular Biology Reviews* **77**: 342–356.

Newcombe G, Stirling B, McDonald S, Bradshaw HD. **2000**. *Melampsora × columbiana*, a natural hybrid of *M. medusae* and *M. occidentalis*. *Mycological Research* **104**: 261–274.

Oksanen J, Blanchet FG, Friendly M, Kindt R, Legendre P, McGlinn D, Minchin PR, O'Hara RB, Simpson GL, Solymos P, *et al.* 2017. Package 'vegan' | Community Ecology Package. : 1–292.

Orrock JL, Fletcher Jr. RJ. **2005**. Changes in community size affect the outcome of competition. *The American Naturalist* **166**: 107–111.

Palmgren A. **1926**. Chance as an element in plant geography. In: Duggar B, ed. Proceedings of the International Congress of Plant Sciences. Ithica, New York, 591–602.

Peay KG, Belisle M, Fukami T. **2012**. Phylogenetic relatedness predicts priority effects in nectar yeast communities. *Proceedings of the Royal Society B: Biological Sciences* **279**: 749–758.

Quinn TP, Erb I, Richardson MF, Crowley TM. **2018**. Understanding sequencing data as compositions: an outlook and review. *Bioinformatics* **34**: 2870–2878.

Redford AJ, Bowers RM, Knight R, Linhart Y, Fierer N. **2010**. The ecology of the phyllosphere: geographic and phylogenetic variability in the distribution of bacteria on tree leaves. *Environmental Microbiology* **12**: 2885–2893.

Reisberg EE, Hildebrandt U, Riederer M, Hentschel U. **2013**. Distinct phyllosphere bacterial communities on *Arabidopsis* wax mutant leaves. *PLoS ONE* **8**: e78613.

Schindelin J, Arganda-Carreras I, Frise E, Kaynig V, Longair M, Pietzsch T, Preibisch S, Rueden C, Saalfeld S, Schmid B, *et al.* 2012. Fiji: an open-source platform for biological-image analysis. *Nature Methods* **9**: 676–682.

Schlaeppi K, Bulgarelli D. **2015**. The plant microbiome at work. *Molecular Plant-Microbe Interactions* **28**: 212–217.

Sinha R, Abu-Ali G, Vogtmann E, Fodor AA, Ren B, Amir A, Schwager E, Crabtree J, Ma S, Abnet CC, *et al.* 2017. Assessment of variation in microbial community amplicon sequencing by the Microbiome Quality Control (MBQC) project consortium. *Nature Biotechnology* **35**: 1077–1086.

Smithson M, Verkuilen J. **2006**. A better lemon squeezer? Maximum-likelihood regression with beta-distributed dependent variables. *Psychological Methods* **11**: 54–71.

Somervuo P, Koskinen P, Mei P, Holm L, Auvinen P, Paulin L. **2018**. BARCOSEL: a tool for selecting an optimal barcode set for high-throughput sequencing. *BMC Bioinformatics* **19**: 257.

Spence C, Alff E, Johnson C, Ramos C, Donofrio N, Sundaresan V, Bais H. **2014**. Natural rice rhizospheric microbes suppress rice blast infections. *BMC Plant Biology* **14**: 130.

Stevens JL, Jackson RL, Olson JB. **2013**. Slowing PCR ramp speed reduces chimera formation from environmental samples. *Journal of Microbiological Methods* **93**: 203–205.

Sturm M, Schroeder C, Bauer P. **2016**. SeqPurge: highly-sensitive adapter trimming for paired-end NGS data. *BMC Bioinformatics* **17**: 208.

Sutherland JP. **1974**. Multiple stable points in natural communities. *The American Naturalist* **108**: 859–873.

Team RC. **2019**. R: A language and environment for statistical computing.

Tuskan GA, DiFazio S, Jansson S, Bohlmann J, Grigoriev I, Hellsten U, Putnam N, Ralph S, Rombauts S, Salamov A, *et al.* 2006. The genome of Black Cottonwood, *Populus trichocarpa* (Torr. & Gray). *Science* **313**: 1596–1604.

Untergasser A, Cutcutache I, Koressaar T, Ye J, Faircloth BC, Remm M, Rozen SG. **2012**. Primer3—new capabilities and interfaces. *Nucleic Acids Research* **40**: e115–e115.

Vandenkoornhuyse P, Quaiser A, Duhamel M, Le Van A, Dufresne A. **2015**. The importance of the microbiome of the plant holobiont. *New Phytologist* **206**: 1196–1206.

Vannette RL, Fukami T. **2014**. Historical contingency in species interactions: towards niche-based predictions. *Ecology Letters* **17**: 115–124.

Venables WN, Ripley BD. **2002**. *Modern Applied Statistics with S*. Springer New York.

Vorholt JA, Vogel C, Carlström CI, Müller DB. **2017**. Establishing causality: opportunities of synthetic communities for plant microbiome research. *Cell Host & Microbe* **22**: 142–155.

Wallace JG, Kremling KA, Kovar LL, Buckler ES. **2018**. Quantitative genetics of the maize leaf microbiome. *Phytobiomes Journal* **2**: 208–224.

Wang Y, Naumann U, Wright S, Warton D. **2019**. mvabund: statistical methods for analysing multivariate abundance data.

Warton DI. **2011**. Regularized sandwich estimators for analysis of high-dimensional data using generalized estimating equations. *Biometrics* **67**: 116–123.

Warton DI, Thibaut L, Wang YA. **2017**. The PIT-trap—A "model-free" bootstrap procedure for inference about regression models with discrete, multivariate responses. *PLOS ONE* **12**: e0181790.

Van Wees SC, Van der Ent S, Pieterse CM. **2008**. Plant immune responses triggered by beneficial microbes. *Current Opinion in Plant Biology* **11**: 443–448.

Weighill D, Jones P, Shah M, Ranjan P, Muchero W, Schmutz J, Sreedasyam A, Macaya-Sanz D, Sykes R, Zhao N, *et al.* 2018. Pleiotropic and epistatic network-based discovery: integrated networks for target gene discovery. *Frontiers in Energy Research* **6**: 1–20.

Werner GDA, Kiers ET. **2015**. Order of arrival structures arbuscular mycorrhizal colonization of plants. *New Phytologist* **205**: 1515–1524.

Wright, Erik S. **2016**. Using DECIPHER v2.0 to analyze big biological sequence data in R. *The R Journal* **8**: 352.

Zahn G, Amend AS. **2017**. Foliar microbiome transplants confer disease resistance in a critically-endangered plant. *PeerJ* **5**: e4020.

Zamioudis C, Pieterse CMJ. **2012**. Modulation of host immunity by beneficial microbes. *Molecular Plant-Microbe Interactions* **25**: 139–150.

Zeileis A, Hothorn T. **2002**. Diagnostic checking in regression relationships. *R News* **2**: 7–10.

Zhang B, Zhu W, Diao S, Wu X, Lu J, Ding C, Su X. **2019**. The Poplar pangenome provides insights into the evolutionary history of the genus. *Communications Biology* **2**: 215.

Figure 1: Average fungal species composition in the *P. trichocarpa* foliar microbiome depends on both (a) species arrival order and (b) host genotype. Colored points show the group means (± sd) for the first 2 constrained axes of partial distance-based redundancy analyses using Jensen-Shannon distance. Each ordination shows the effect of one factor, species arrival order or host genotype, after controlling for the effect of the other. Point colors indicate (a) which fungal species was the initial colonist in the species arrival order treatments, or (b) whether the host genotype originated east or west of the Cascade Divide.

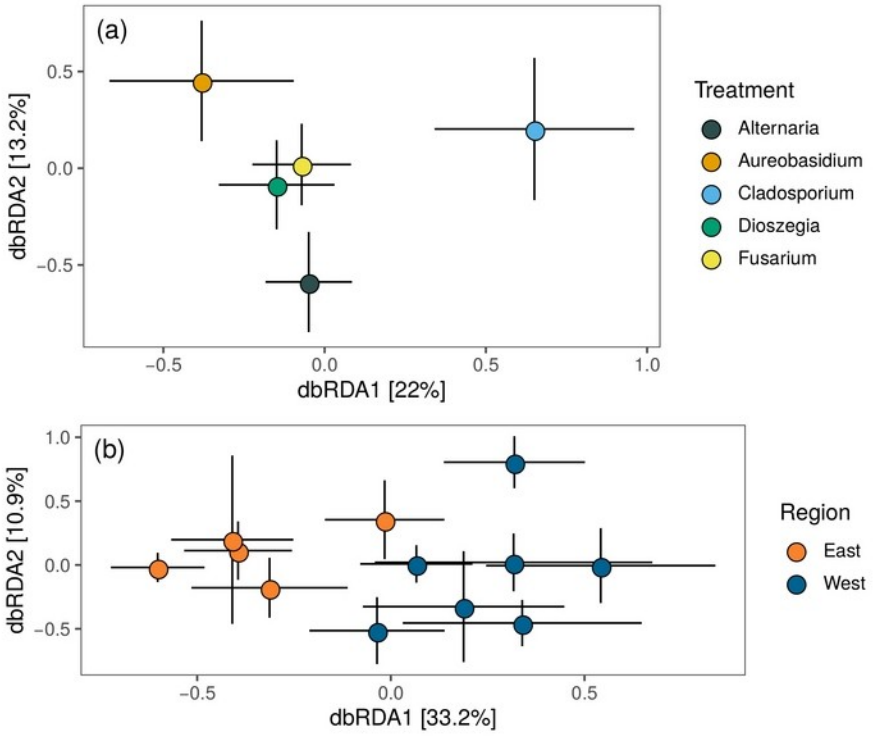

Figure 2: Individual members of the 8-species synthetic fungal community varied in their response to arrival order (Treatment) and host genotype. Species are ordered, top to bottom, from most to least abundant in the sequence data, and bold names indicate species that were initial colonists in one of the arrival order treatments. Color indicates the partial pseudo-r^2 for each model term in univariate negative-binomial glms, calculated following the method of Nagelkerke (1991). Symbols indicate the significance (permutation tests) of individual species' contributions to the multivariate (community-level) response, calculated using step-down resampling to account for multiple testing, where $^{+}P < 0.1$, $^{*}P < 0.05$, $^{**}P < 0.01$, and $^{***}P < 0.001$.

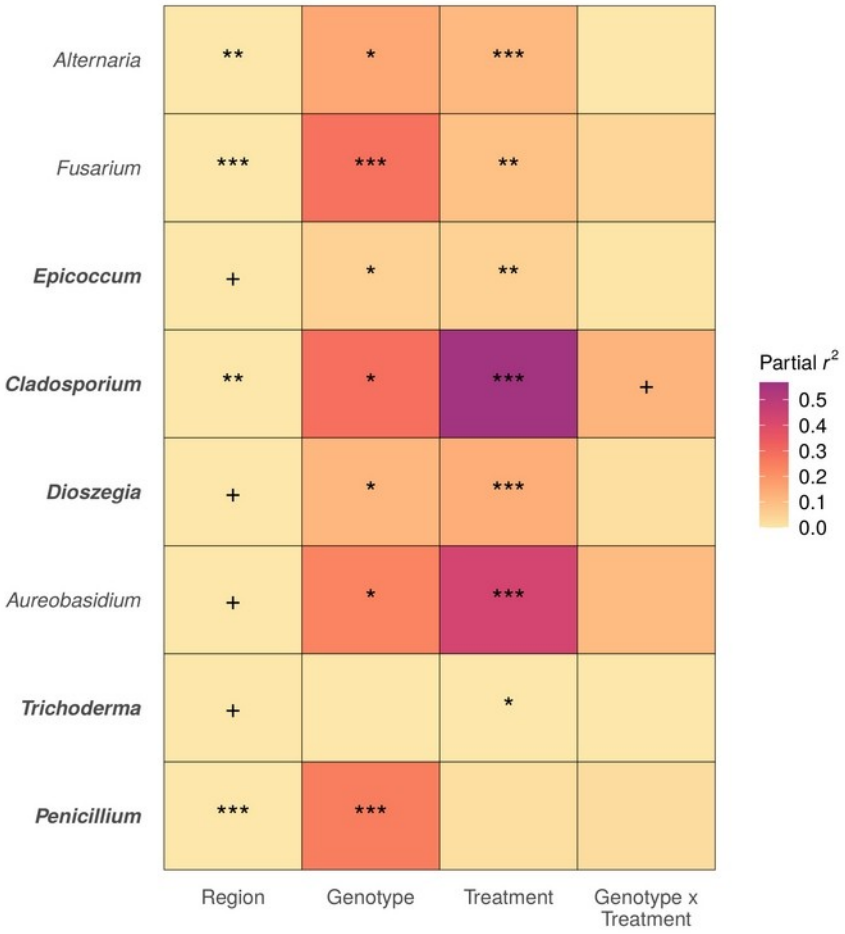

Figure 3: The advantage of preemptive colonization in the *P. trichocarpa* foliar microbiome depends on species identity (panels a-e) and the host genotype (point colors), but not the geographic origin of the host (inset plots). The strength of priority effects for each species on each genotype was calculated as the log ratio of the relative abundance when arriving first vs. arriving concurrent with the community. Points show the observed priority effect for each species on each plant genotype and the black bars show the 95% bootstrap confidence intervals (bias-corrected and accelerated). Insets show bootstrap distributions of the mean strength of priority effects for each species on host genotypes originating east or west of the Cascade Divide. Significant mean priority effects, based on bootstrapped one-sample t-tests, are indicated, where $^{*}P < 0.05$, $^{**}P < 0.01$, and $^{***}P < 0.01$.

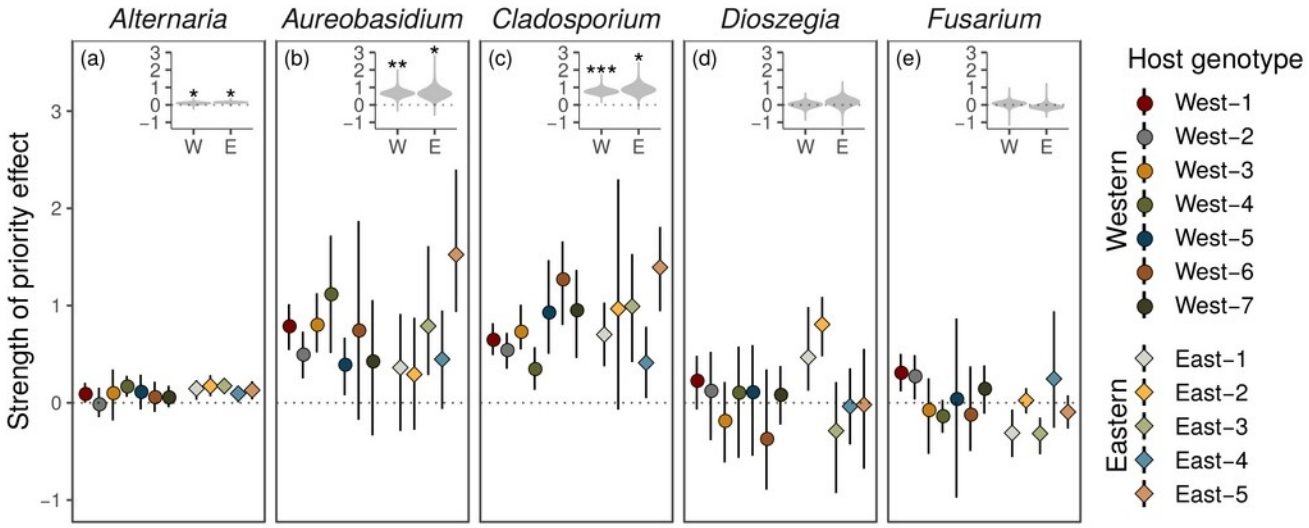

Figure 4: Priority effects during fungal community assembly in the *P. trichocarpa* foliar microbiome affects the severity of *Melampsora* leaf rust in rust susceptible plant genotypes. Large points indicate the estimated marginal means (± 95% CIs) from beta-regression models. Small points show individual rust severity observations (% leaf area with chlorotic lesions) for each species arrival order treatment (colors) on each host genotype (panels). Transparency of small points indicate the weight used (number of individual leaves measured per plant) in the beta-regression models. Horizontal dotted lines indicate the mean rust severity in uninoculated control plants.

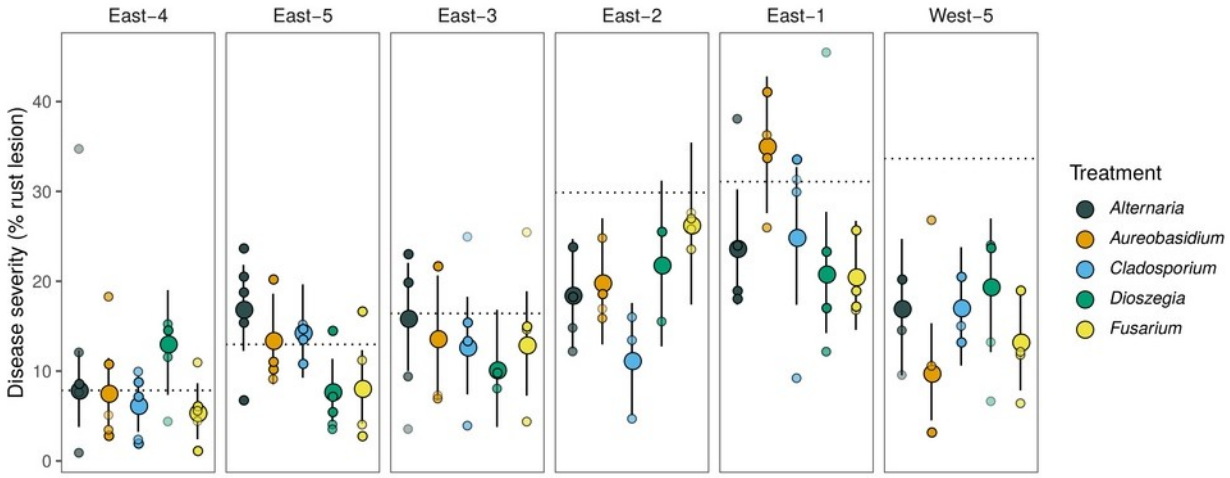

Table 1: Results of multivariate, negative-binomial generalized linear models, testing whether fungal species composition in the *P. trichocarpa* foliar microbiome varies with species arrival order treatments, and whether these effects vary among (a) individual plant genotypes, or (b) populations of plant genotypes separated by the Cascade Divide (ie., region).

(a) Genotype-level model

Predictor	**Δdf**	**Residual df**	**Wald-χ^2**	***P*-value**
Genotype	11	235	20.2	< 0.001***
Treatment	4	231	21.8	< 0.001***
Genotype:Treatment	44	187	23.5	0.038*

(b) Region-level model

Predictor	**Δdf**	**Residual df**	**Wald-χ^2**	***P*-value**
Region	1	245	12.4	< 0.001***
Treatment	4	241	21.7	< 0.001***
Region:Treatment	4	237	6.16	0.31

Table 2: Results of likelihood ratio tests comparing beta-regression models of rust severity for either (a) rust susceptible or (b) rust resistant *P. trichocarpa* genotypes.

(a) Rust susceptible genotypes

Predictor	**Δdf**	**LRT-χ^2**	***P*-value**
Genotype	5	60.2	< 0.001***
Treatment	4	4.53	0.34
Genotype:Treatment	20	33.6	0.03*

Full model: N = 117; pseudo-r^2 = 0.47; DF = 86

(b) Rust resistant genotypes

Predictor	**Δdf**	**LRT-χ^2**	***P*-value**
Genotype	5	33.5	< 0.001***
Treatment	4	1.74	0.78
Genotype:Treatment	20	5.95	0.99

Full model: N = 125; pseudo-r^2 = 0.24; DF = 89